NTU Journal of Engineering and Technology (2025) 4 (4): 39 - 58
DOI: https://doi.org/10.56286/ntujet.v4i4

IRAQI Academic Scientific Journals

P-ISSN: 2788-9971 E-ISSN: 2788-998X
NTU Journal of Engineering and Technology
Available online at: https://journals.ntu.edu.iq/index.php/NTU-JET/index

Electroretinography: A Comparative Study of Modalities and Analytical Approaches with Partial Integration of OCT Findings

Mayada Fares Alhamamy[1], Mohammed Sabah Jarjees [2], Wan Zuha Wan Hasan[3]
[1]Department of Medical Instrumentation Techniques Engineering, Technical Engineering College of Mosul, Northern Technical University, Mosul, Iraq,
[2]Department of Medical Instrumentation Techniques Engineering, Technical Engineering College of Mosul, Northern Technical University, Mosul, Iraq,
[3]Department of Electrical and Electronic Engineering, Faculty of Engineering, University Putra Malaysia.
mayada.fares@ntu.edu.iq, mohammed.s.jarjees@ntu.edu.iq, wanzuha@upm.edu.my

Article Informations

Received: 24-09- 2025,
Revised: 20-10-2025,
Accepted: 26-10-2025,
Published online: 28-12-2025.

Corresponding author:
Name: Mayada F. Alhamamy
Affiliation: Northern Technical University
Email: mayada.fares@ntu.edu.iq

Key Words:
Electroretinography (ERG),
optical coherence tomography (OCT),
feature extraction,
time–frequency analysis.

A B S T R A C T

Electroretinography (ERG) is an essential tool for assessing retinal function, with responses from photoreceptors, ganglion cells, and inner layers. Clinical applications are often secondary to structural imaging, though dysfunction may appear before anatomical changes. This review compares three ERG types: full-field (ffERG), patterned (PERG), and multifocal (mfERG), highlighting differences in response, waveform components, and clinical uses. This review analyzes more than 60 studies (2014–2025). Advanced analyses in the time, frequency, and time–frequency domains demonstrated diagnostic accuracies between 85% and 97% for early detection of retinal dysfunctions such as glaucoma and retinitis pigmentosa. Integrating ERG with Optical Coherence Tomography (OCT) improved structure–function correlation by 15–25%. The findings highlight that combining ERG with quantitative feature extraction and OCT enhances early diagnosis and monitoring of retinal diseases and supports standardized clinical applications.

1. Introduction

Retinal and optic-nerve diseases are among the leading causes of visual impairment and blindness worldwide, making reliable and accurate diagnostic tools crucial in clinical practice [1]. Electroretinography (ERG) and optical coherence tomography (OCT) are key modalities in this field: ERG provides a functional assessment of retinal activity, while OCT delivers high-resolution structural measurements of retinal tissues [2]. Recent studies have shown that combining ERG and OCT yields a more comprehensive integrated assessment [3,4]. Moreover, ERG signal analysis has evolved from traditional time-domain measurements (e.g., amplitude and latency) to more advanced techniques in the frequency and time–frequency domains, enabling extraction of more sensitive and reliable biomarkers. This review first outlines the physiological basis of the retina to facilitate interpretation of ERG components, then summarizes ERG types, discusses their integration with OCT, and evaluates signal-analysis methodologies across time, frequency, and time–frequency domains, emphasizing clinical applications and future challenges. Previous reviews have focused on specific ERG modalities or on individual diseases (e.g., inherited retinal disorders [5], glaucoma [6], or OCT-based monitoring in dry age-related macular degeneration (AMD) [7]. However, none systematically compared ERG analytical domains (time, frequency, time–frequency) or integrated them with OCT. Our review fills that gap by providing a comprehensive synthesis across ERG modalities, highlighting complementary diagnostic insights and proposing directions for future multimodal and AI-driven research.

2. Physiological Basis of ERG

The retina is a light-sensitive layered structure covering the back of the eye, as shown in Figure ١. It serves as an integral part of the visual system and maintains close anatomical and physiological connections with the brain[8] .When a light stimulus is presented to it, the retina responds by converting light into nerve signals. These responses reflect the functional integrity of different retinal layers, primarily the photoreceptors and bipolar cells. When photons reach the retina, they are converted into neural signals through a process called phototransduction. In the dark, photoreceptors maintain a depolarized state due to the influx of cations through Cyclic Guanosine Monophosphate (cGMP) gated channels, known as the “dark current.” Upon exposure to light, activation of rhodopsin triggers a G-protein cascade, resulting in the closure of these channels and subsequent hyperpolarization of the photoreceptors. This hyperpolarization is recorded as the a-wave, a negative deflection in the ERG signal. Following photoreceptor activation, ON bipolar cells respond to decreased glutamate release by depolarizing, generating a positive b-wave, representing inner retinal activity. These two main components, the a-wave and b-wave, form the basis for interpreting the flash ERG [9].

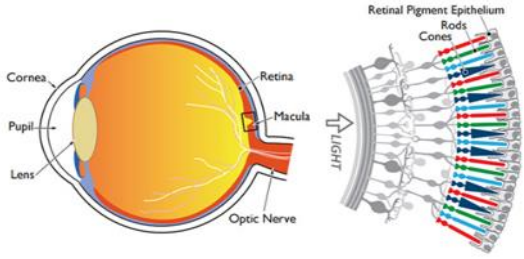

Fig. 1. Drawing of a section through the human eye with a schematic enlargement of the retina. From reference [10].

3. ERG Modalities

Various ERG methods have been developed to assess retinal function. ERG is a non-invasive electrophysiological technique [11]. ERG reflects the functions of photoreceptors and the inner nuclear layers of the retina [١٢,١٣,١٤]. It is also considered the first biopotential ever recorded in a human, specifically by Dewar in 1877 [15]. Depending on the type of light stimulus and the initial state of adaptation to the background, a specific retinal layer, a localized region, or the entire retina can be stimulated to produce various types of responses, such as patterned ERG (PERG), multifocal ERG (mfERG) [16,17], full-field ERG (ffERG) [١٨] focal ERG (fERG), These methods are important tools for early detection and diagnosis of a wide range of retinal diseases, such as early diabetic retinopathy, glaucoma, macular degeneration, and age-related macular degeneration [19,20].

3.1 Multifocal ERG

The mfERG is one of the most widely used procedures for measuring local retina function. It generates a detailed topographic map of electrical activity in various parts of the retina, particularly the central retina, at an angle of around 45 to 60°. This technique relies on stimulating specific regions of the retina with a hexagonal stimulus, typically presented as an array containing 61 or 103 elements Figure ٢. Each hexagon can take two states, light and dark, i.e., on and off. It changes rapidly between these two states, driven by a predetermined ‘‘pseudorandom’’ binary sequence (m-sequence) [16]. mfERG is recorded under light-adapted

conditions and specifically targets the cone-driven retina. The resulting waveform has three major components: N1 (the initial negative component), P1 (the positive component), and N2. N1 represents the responses of cones and their bipolar cells, whereas P1 and N2 are assumed to represent the activity of bipolar cells and subsequent processes within the retina [21,22]. mfERG analysis relies on cross-correlation between the stimulus sequence and the continuous electrical signal recorded at the corneal surface, enabling the isolation of the electrical response from each retinal location. This results in a multilevel analysis known as kernels, which include first-order kernels, which reflect the direct response to the stimulus, and second-order kernels, which reflect the superposition of the effects of successive stimuli [23,24].mfERG was developed to overcome this limitation [24,25]. mfERG is utilized in clinical settings to detect or rule out malfunction in certain parts of the retina, particularly those involved with cones and bipolar cells. It is a valuable tool for early diagnosis of localized retinal diseases such as macular degeneration and cone-dependent disorders [16]. Compared to ffERG, mfERG has greater stimulation rates and offers exact positional information regarding retinal performance, which aids in the diagnosis of localized pathological problems that conventional radiography does not detect. Therefore, mfERG is a vital tool in detecting early changes associated with degenerative or localized diseases in the central retina [26,27].

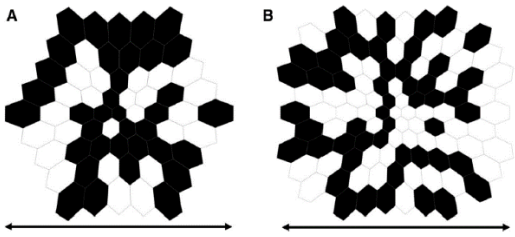

Fig. 2. depicts typical mfERG stimuli consisting of hexagonal pieces that grow in size with eccentricity. The stimulus array is composed of either 61 or 103 elements. In standard mfERG recordings, the horizontal extent of the stimulus array covers approximately 40° to 50° of the visual field [16].

3.2 Pattern ERG

The PERG is a technique used to assess the function of retinal ganglion cells (RGCs) and photoreceptors in the central macula. Unlike whole-mount ffERG, which stimulates the entire retina, PERG focuses on the central area only and therefore has a low amplitude response. PERG requires recording iterations, sometimes over 100 times, to improve the signal-to-noise ratio [٢٩,٣٠].PERG is typically elicited using alternating visual patterns, such as checkerboard or successive stripes [٣٠], where the light pattern is periodically reversed to produce structured visual stimulation. PERG recording requires precise visual fixation from the patient. The stimulus field can be expanded from 15° to 30° to assess the paracentral region if fixation is not possible. This is a practical alternative to mfER [17] .The transient PERG pattern is the most widely used clinical standard and consists of three main components: N35 (initial negative deviation), P50 (positive peak at 50 ms), and N95 (negative peak at 95 ms) [17]. As shown in Figure 3 . P50 is used as an indicator of the integrity of photoreceptors in the central macula and inner retina, i.e., it reflects the function of the pre-neural macula, while N95 is considered to be related to the function of ganglion cells and the optic nerve and is significantly influenced by the degree of visual contrast [17,29]. Steady-state PERG (SS-PERG) is produced when high inversion frequencies (>10 inversions/s) are used, and the resulting waveform is sinusoidal with constant shape and amplitude, making it suitable for frequency domain analysis. [35,36,37].Some studies suggest that SS-PERG may be more sensitive for early detection of optic nerve damage, such as in glaucoma, than transient responses [33].

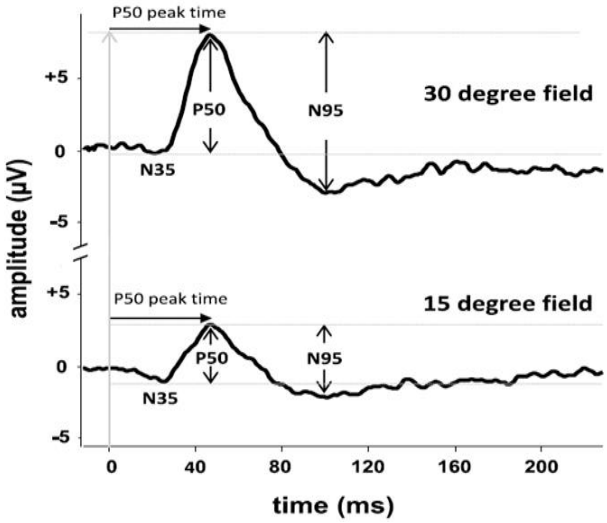

Fig. 3. Pattern ERG waveforms. Pattern ERGs recorded to 50' check widths presented in standard 15-degree and 30-degree fields. The PERG P50 peak times from the 30 and 15-degree fields are the same, but the P50 amplitude is large [17].

3.3 The full-field ERG

The ffERG is a block potential that reflects the overall electrical activity of the retina. ffERG is an established clinical technique for assessing overall retinal function [35,36]. It involves stimulating the entire retina with a short-duration, homogeneous flash of light, typically lasting less than 5 milliseconds, as defined by the International Society for Clinical Electrophysiology of Vision (ISCEV) [32]. Figure 4 shows six steps of the clinical ffERG as part of a protocol widely accepted as an international clinical protocol. Standard and defined

by ISCEV [14,36] . Depending on the adaptation conditions (scotopic or photopic) and flash intensity, ffERG can selectively assess rod or cone system function. Under dark-adapted (scotopic) conditions, dim flashes (e.g., DA 0.01 cd·s/m²) primarily elicit responses from rod bipolar cells, while brighter flashes (DA 3.0 or DA 10.0) produce mixed rod-cone responses [37,38,39]. In light-adapted (photopic) conditions, the single-flash (LA 3.0 cd·s/m²) and 30 Hz flicker stimuli are used to assess cone system function, with the latter being particularly sensitive [40,41]. The typical ffERG waveform consists mainly of two components: the a-wave, a negative deflection representing photoreceptor (rod and cone) hyperpolarization [37], and the b-wave, a positive deflection generated mainly by ON-bipolar cells, with additional contributions from Müller cells and other inner retinal neurons [36]. Additional components include oscillatory potentials (OPs), believed to originate from inner retinal feedback circuits involving amacrine cells [38,39], and the photopic negative response (PhNR), which reflects ganglion cell function under photopic conditions [40] .The i-wave, seen under photopic conditions following the b-wave, is less understood and may involve off-bipolar cell activity [38] .Clinically, ffERG is used to detect and differentiate various inherited retinal dystrophies, such as cone-rod or rod-cone dystrophies, and can guide genetic diagnosis [41,42]. However, a notable limitation of ffERG is its inability to detect localized retinal dysfunction, as the response reflects a mass signal from the entire retina.

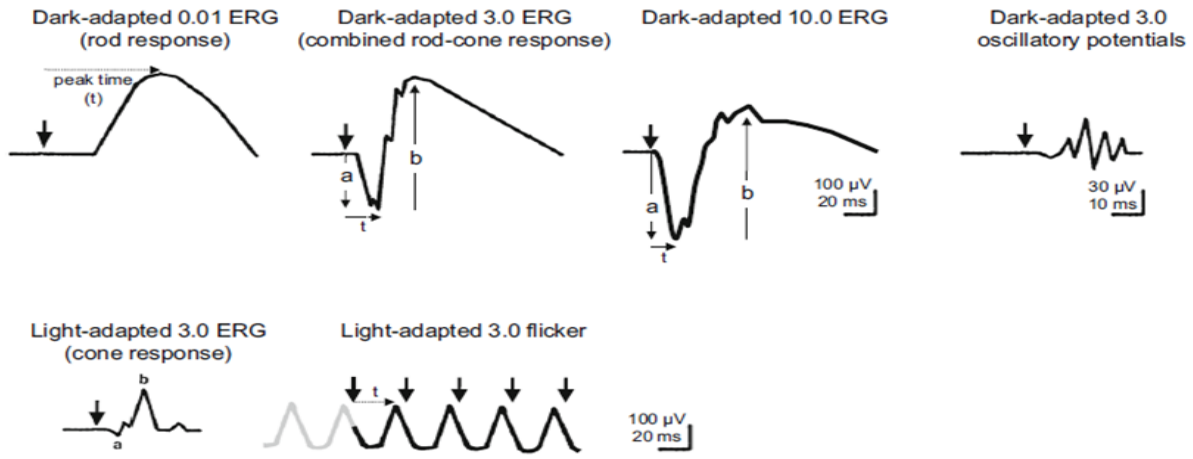

Fig. 4. diagram depicts the six recording conditions established by the ffERG ISCEV Standard. Bold arrowheads mark the stimulus flashes, solid arrows indicate the a- and b-wave amplitudes, and dotted arrows demonstrate the method for measuring time-to-peak (t, implicit time, or peak time).From reference [34].

To clarify the differences between the different types of electroretinography in an organized manner, the most important clinical and technical characteristics of each type were summarized in Table 1, while Figure ٥ shows the waveforms and visual stimuli characteristic of each.

Understanding the distinct physiological and technical characteristics of each ERG modality provides a foundation for integrating these signals with structural imaging techniques such as OCT, which enhances diagnostic interpretation through a combined structure–function approach.

4. OCT–ERG Integration

OCT, particularly advanced forms such as spectral-domain OCT (SD-OCT) and Optical coherence tomography angiography (OCTA), are essential tools for detecting structural and microvascular changes in the retina and optic nerve [51]. SD-OCT provides high-resolution cross-sectional images that allow for accurate measurements of retinal thickness and morphological changes, while OCTA enables non-invasive imaging of microvasculature in the retina and choroid [٤٤]. These techniques are particularly valuable in diseases such as diabetic retinopathy, glaucoma, and even neuropsychiatric disorders like schizophrenia [45]. simultaneous acquisition of structural and functional metrics and illustrating the structure–function relationship as shown in Figure 6. .Recent studies have demonstrated that structural parameters obtained from OCT, such as Retinal Nerve Fiber Layer (RNFL) and Ganglion Cell–Inner Plexiform Layer (GCIPL) thickness, show strong correlations with ERG functional parameters, including N95 and P50 amplitudes [46,47].For example, reduced RNFL thickness is frequently associated with a decrease in N95 amplitude in PERG, indicating early retinal ganglion cell dysfunction even before visual field defects appear [54].

Table 1. Comparison of the main ERG variants in terms of purpose, stimulation, waveform components, recording conditions, clinical applications, and limitations.

Feature	ffERG	PERG	mfERG
Purpose	Global retinal function	Central retina, RGCs	Local retinal function (macula ± periphery)
Stimulus Type	Flash of light	Contrast-reversing checkerboard	61 Hexagon array (pseudorandom pattern)
Waveform Components	a-wave, b-wave, OPs, PhNR	N35, P50, N95	N1, P1, N2
Amplitude	Large	Low	Moderate (depends on retinal area)
Area Stimulated	Entire retina	Central 15–30°	Central 45–60° regions
Recording Conditions	Dark- and light-adapted	Requires fixation; repeated averaging	Light-adapted, pseudorandom stimulation
Clinical Uses	Assessing overall retinal function; diagnosing widespread retinal diseases such as retinitis pigmentosa and diabetic retinopathy.	Early detection of optic nerve diseases and glaucoma; monitoring retinal ganglion cell damage.	Diagnosing and monitoring central retinal diseases such as AMD and diabetic retinopathy; evaluating localized retinal areas.
Limitations	- Does not identify specific areas of the retina. - Insensitive to early detection.	Measures only retinal ganglion cells. - Sensitive to eye movement. - Requires a special visual pattern.	Covers only a central area.

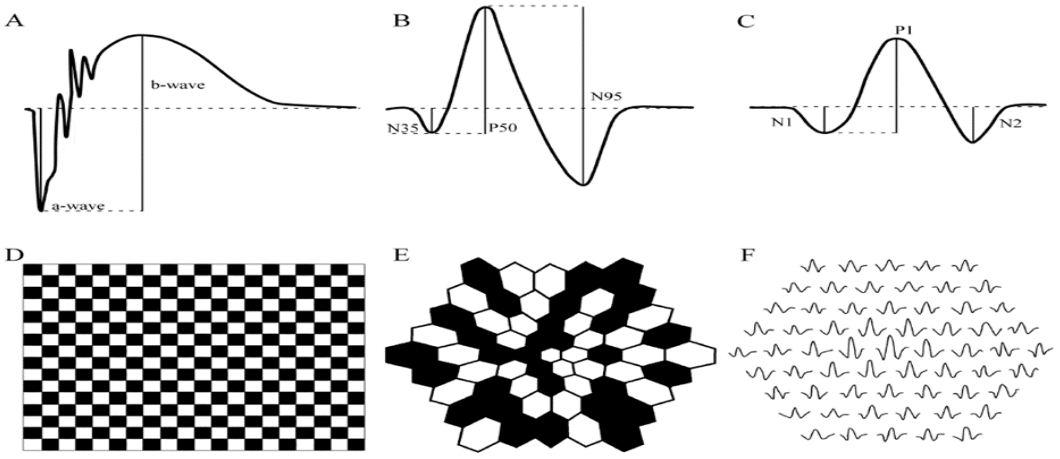

Fig. 5. Schematic waveforms of the three main types of ERG. (A) ffERG waveform with the a-wave and b-wave. (B) PERG waveform with N35, P50, and N95. (C) mfERG waveform showing N1, P1, and N2. (D) Checkerboard stimulus for PERG. (E) 61-wave hexagonal pattern for mfERG. (F) Matrix of 61 positional responses for mfERG [43].

Similarly, localized reductions in mfERG response density correspond to thinning in the outer retinal layers detected by SD-OCT, suggesting a direct structure–function relationship [59] as shown in Table ۲ for a summary of key studies.This combination method improves diagnostic accuracy, allows for earlier diagnosis of disease development, and facilitates more precise monitoring and personalized therapy options in retinal and optic nerve disorders.

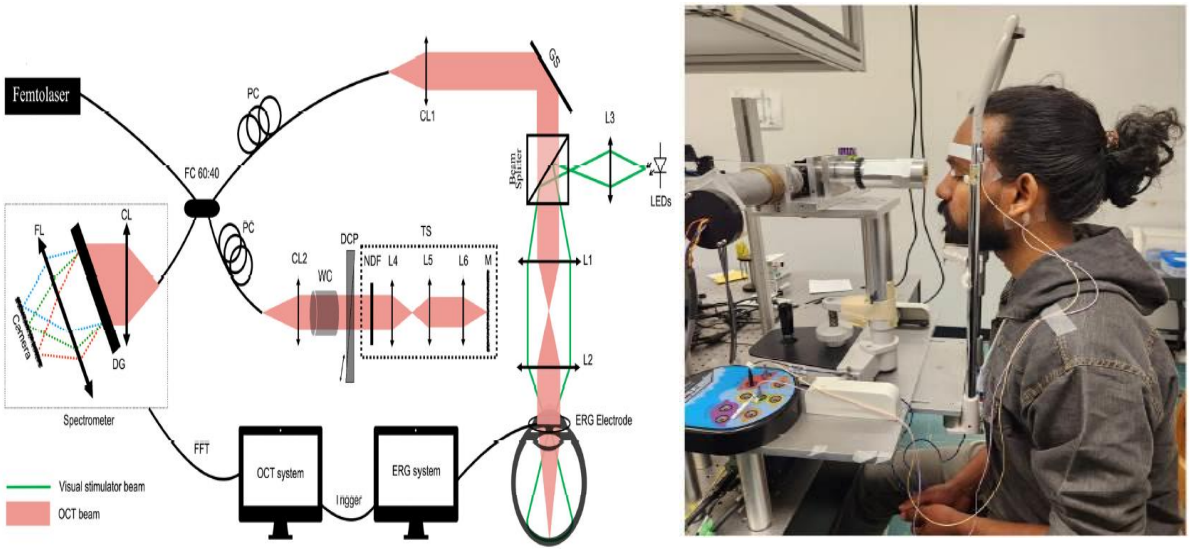

Fig. 6. (a) Schematic for the integrated OCT+ERG system. (b) A photograph of the OCT+ERG imaging probe. This method allows for simultaneous assessment of retinal structure (by OCT) and function (via ERG), demonstrating the structure-function link in retinal and optic nerve disorders [48].

Table 2. summarizes recent studies that have used OCT in conjunction with several ERG modalities, their clinical uses, and the reported benefits of this multimodal strategy.

Year [Ref]	Disease	Method (OCT + ERG)	No. of Subjects	Main Findings / Benefits
2015 [46]	Glaucoma	SS-PERG + SD-OCT	24 glaucoma + 25 controls	Coefficient of Variation (CV) phase in PERG showed high sensitivity for detecting retinal ganglion cell dysfunction before RNFL thinning or standard automated perimetry (SAP) defects.
٢٠١٦ [49]	AMD	mfERG + SD-OCT	Not available	Functional changes mfERG preceded structural changes (SD-OCT), enabling early diagnosis and treatment.
٢٠١٧ [50]	Glaucoma	SS-PERG + SD-OCT	90 eyes (48 glaucoma, 42 controls)	Demonstrated a clear structure–function relationship, improving understanding of glaucoma development.
٢٠١٨ [51]	Parkinson's disease	mfERG + SD-OCT	58 patients + 30 controls	Improved diagnostic accuracy by linking retinal structural and functional changes; useful for early diagnosis and monitoring progression.
٢٠٢٠ [52]	Diabetic retinopathy	mfERG + SD-OCT + OCTA	44 diabetic + 18 controls	Identified early vascular and retinal changes before clinical signs of retinopathy appeared.
٢٠٢١ [47]	Retinitis pigmentosa	SS-PERG + SD-OCT	188 eyes (90 typical, 74 paracentral, 24 others)	Strong correlation between OCT and ERG, useful for predicting visual acuity and monitoring progression.
٢٠٢١ [53]	Normal-Tension Glaucoma(NTG)	PERG + SD-OCT + OCTA	109 eyes (49 healthy, 60 NTG)	Early detection of ganglion cell dysfunction; OCTA added microvascular and structural insights.
٢٠٢١ [54]	Glaucoma	PERG + SD-OCT	72 glaucoma patients	Detected retinal ganglion cell dysfunction before visual field defects.
٢٠٢٣ [55]	Schizophrenia spectrum disorders	ffERG + SD-OCT	12 studies, 250 patients	Revealed strong structure–function correlations in retina, suggesting retina as a biomarker for diagnosis and follow-up.
٢٠٢٤ [56]	Preperimetric glaucoma	High-Frequency - PERG + SD-OCT	65 eyes (33 preperimetric, 32 controls)	HF-N95 ratios correlated GCIPL thickness; half-analysis improved sensitivity for early diagnosis.
٢٠٢٥ [57]	Pediatric optic neuropathy	PERG + Pattern Visual Evoked Potential (PVEP) + SD-OCT	42 patients + 42 controls	Allowed early detection of structural and functional changes in children; useful when the OCT imaging quality is limited.

As summarized in Table 2, integrating OCT with various ERG modalities has consistently demonstrated improved diagnostic precision and structure–function correlation. Studies across glaucoma, diabetic retinopathy, AMD, and neuro-ophthalmic disorders revealed that combining functional and structural assessments enhances early disease detection by 15–25% and provides valuable insight into retinal ganglion and photoreceptor integrity. This multimodal approach strengthens clinical decision-making and supports more personalized monitoring strategies compared with standalone techniques.

While OCT integration bridges the gap between structural and functional evaluations, advanced analytical techniques are equally essential for quantifying ERG signals. The following sections present various signal processing methods applied to ERG data, illustrating how each analytical domain contributes to extracting meaningful diagnostic information.

5. Analytical Domains (Time, Frequency, Time–Frequency)

The ERG waveform can be studied in a variety of domains, including time, frequency, and time-frequency, to determine the signal's function. Figure 7 presents the block diagram depicts multiple studies for ERG signals based on three categories and consolidates the number of papers accessible in the literature for each category.

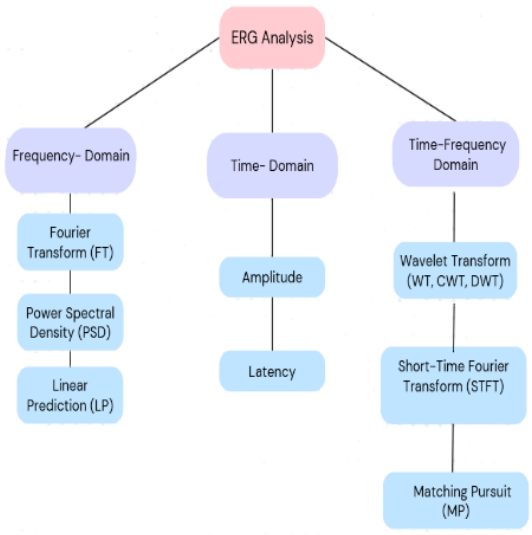

Fig. 7. A block diagram based on multiple analyses that shows ERG research.

5.1 Time-domain analysis

Because they are relatively easy to interpret, time-domain features are widely used by clinicians, extracting information and characteristic features directly from the signal itself rather than converting it to another domain. This type of analysis focuses primarily on two key parameters: amplitude, which reflects the intensity of the electrical response, and implicit time (latencies), which is the time interval between the onset of a stimulus and the peak of each wave. Amplitudes and implicit times are used to determine the evaluation of retinal changes, distinguish between responses of healthy and unhealthy individuals, and monitor changes resulting from medical or surgical treatment [58]. As a result, they are among the most widely used metrics in ERG research and are regularly used as benchmarks for evaluating various signal processing approaches. Time-domain features are clinically important and easy to understand, but they are susceptible to artifacts, which can make them less accurate. Moreover, time-domain features have lower computational complexity than frequency-domain features, as they depend directly on the signal amplitude and its temporal relation, whereas frequency-domain features require transforming the signal using methods such as the Fast Fourier Transform (FFT)[59]. Consequently, various studies recommend combining these features with those from other domains, such as frequency or time–frequency, to improve analytical reliability [59,60] . Additionally, the FFT algorithm can be applied to analyze the signal in the frequency domain, with the possibility of reconstructing the original signal using the inverse Fourier transform under certain conditions [25]. Figure 8 represents a visualization of the basic temporal parameters extracted from the ERG signal, while Table 3 provides a compilation of all time-domain investigations performed on different ERG response.

Fig. 8. A typical ERG from a visually normal subject is shown. In this figure, variables, including: a-wave amplitude, b-wave amplitude, and PhNR. t1: a-wave implicit time; t2: b-wave implicit time, t3: PhNR implicit time [24].

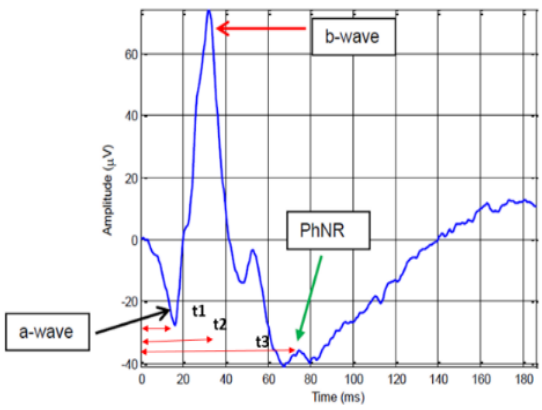

Table 3. A compilation of all Time-domain investigations performed on all ERG responses.

Year [Ref]	Signal /Stimulation	No. of Subjects	Features Extracted	Limitations
2014 [61]	mfERG (103 hexagons, 200 cd/m²)	104 (60 AMD, 44 controls)	N1-P1 amplitude, P1 implicit time, retinal sensitivity	mfERG & microperimetry not significantly correlated
٢٠١٥ [62]	Full-field photopic ERG (single-flash, 30 Hz)	171 (151 diabetic, 20 healthy)	B-wave amplitude & peak time, retinal thickness, macular edema	Single time-point, no long-term follow-up, partial control group
٢٠١٦ [63]	PERG	63 (type 1 diabetic, 126 eyes)	PERG & Visual Evoked Potential(VEP) latencies and amplitudes	No healthy comparison, older data, variable testing conditions
2017 [64]	mfERG (103 hexagons, 75 Hz)	40 (20 epiretinal membranes (ERM), 20 healthy)	P1 amplitude density, P1 implicit time	Small sample, categorization accuracy not reported
2017 [65]	PERG	24 Primary Open-Angle Glaucoma (POAG) (11 preperimetric, 13 early)	P50/N95 amplitude & peak time	Small sample size
2018 [66]	Peripheral pattern ERG (PPERG) + conventional PERG	11 healthy	Peripheral ERG function	Difficulty in stimulating the peripheral area accurately
٢٠١٨ [67]	SS-PERG	57 (29 localized, 10 diffuse, 18 normal)	Amplitudes, ratios, visual field sensitivity, RNFL thickness	Visual field & hemifield PERG (h-PERG) differences not correlated; possible fixation & age effects
٢٠٢٠ [68]	ffERG + OCTA	523 eyes (366 diabetic, 157 healthy)	a/b-wave, oscillatory potentials, 30-Hz flicker, vessel density	Peripheral changes not detected; PERG/PhNR not included
٢٠٢٠ [69]	mfERG, PERG, PhNR, SD-OCT	48 participants (92 eyes)	mfERG fovea P1, PERG N95 amplitude/implicit time, PhNR amplitude/implicit time	Small sample, need for OCTA comparison
2021 [70]	ffERG	40	a/b-wave amplitude & peak, Short-Time Fourier Transform (STFT)/continuous Wavelet Transform (CWT)/ discrete-Wavelet Transform (DWT) time-frequency features	Small sample size limits generalizability
٢٠٢٢ [71]	ffERG (dark/light adapted)	60 (28 Retinitis Pigmentosa (RP), 32 healthy)	a/b-wave implicit times, amplitudes, nonlinear features (theta angle, density)	Short ERG signal, variable disease severity
٢٠٢٢ [72] [54]	PERG + PhNR	32 patients	PERG N95, PhNR amplitude, OCT (peripapillary Retinal Nerve Fiber Layer (PRNFL), Ganglion Cell Complex (GCC), Nerve Fiber Layer (NFL))	Inter-visit variability, complex protocols
2023 [73]	PERG + OCT	150 participants (300 eyes)	P50/N95 latency & amplitude, RNFL thickness	Clinical variability in glaucoma assessment
2024 [74]	PERG + Blue-Yellow Visual Evoked Potential (BY-VEP)	412 patients (2571 eyes, 347 analyzed)	PERG amplitude, BY-VEP peak time	No SD-OCT, single measurement, exploratory tests
٢٠٢٥ [75]	mfERG (61 hexagonal stimuli)	96 (77 RP, 19 healthy)	N1/P1/N2 amplitude & latency	Limited to Turkey, time-domain only, further validation needed
2025 [76]	mfERG + Generative Adversarial Network (GAN)Transfer Learning	NA	P1 wave amplitude maps	Overfitting solved by preprocessing & GAN
٢٠٢٥ [77]	Extended Pattern Electroretinography (PERGx, SS-PERG)	60 (20 normal, 20 OHT, 20 Open-Angle Glaucoma(OAG)	PERGx amplitude & phase, delta amplitude & phase angular dispersion	No correlation with RNFL/GCIPL, one eye per participant

5.1.1 Comparison of studies based on time approaches

Studies summarized in Table 3 collectively indicate that time-domain analysis of ERG signals remains a fundamental and widely applied approach for assessing retinal function. Most investigations focused on measuring a- and b-wave amplitudes and implicit times to detect early dysfunction in diseases

such as glaucoma, diabetic retinopathy, and retinitis pigmentosa. Results consistently showed that PERG and mfERG provide sensitive indicators of early ganglion and cone dysfunction, with diagnostic accuracies often exceeding 90%. Recent studies integrating machine learning algorithms, such as ResNet50 and Naive Bayes, achieved classification accuracies above 94%, confirming the potential of AI-assisted ERG analysis as a clinical decision-support tool. However, many studies reported limitations related to small sample sizes and weak correlations between functional and structural measurements, emphasizing the need for broader clinical validation. Frequency domain analysis.

5.2 Frequency domain analysis

Several studies have been performed to analyze the ERG in the frequency domain. This type of analysis uses a variety of techniques to extract frequency components, including the Fourier transform (FT) and the discrete Fourier transform (DFT), as well as some limited methods like empirical mode decomposition (EMD), power spectral density (PSD), and spectrum estimation or linear prediction (LP) [58,78,79,80,81]. Frequency analysis offers more precise measurements of amplitude and peak timings [82]. A compilation of these investigations on different ERG responses is presented in Table 4.

5.2.1 Fourier analysis

Fourier Analysis (FA) is a technique that only operates in the frequency domain. It breaks down a time-domain signal or a given time series into frequency components that together reconstitute the original signal[83]. The Fourier Transform allows you to identify the magnitude or contribution of each frequency in the original signal. In frequency-domain analysis, the first step is to transform the signal from the time domain to the frequency domain using the following technique:

$$X(f) = \int_{-\infty}^{+\infty} x(t) \cdot e^{-2j\pi ft}\, dt \qquad (1)$$

Where X (f) is the signal in the frequency domain and x (t) is the signal in the time domain .The original signal can be reconstructed, under specific conditions, using the inverse Fourier transform. Furthermore, discrete-time implementations of both the forward and inverse Fourier transforms are commonly employed. In practical applications, the transformation in the discrete domain is typically performed using the well-established FFT algorithm.

5.2.2 Power spectral density

PSD is one of the fundamental tools in bio signal analysis, which shows how a signal's energy is divided across frequencies [84,85]. Unlike time-domain analysis, which focuses on amplitude and response time, PSD analysis provides accurate information about a signal's frequency content, allowing for a better understanding of the underlying physiological processes. PSD is used in ERG to derive spectral features from a sample signal, with the energy distribution across frequencies reflecting the functions of various retinal layers [86]. PSD is commonly determined by Fourier processing the signal's autocorrelation sequence [87], which follows the mathematical relationship:

$$S(f) = \int_{-\infty}^{+\infty} r_{xx}(\tau) \cdot e^{-2j\pi ft}\, d\tau \qquad (2)$$

Where $r_{xx}(\tau)$ represents the autocorrelation function, and S (f) denotes the power spectral density [88].

5.2.3 Linear prediction

LP is a time series analysis technique widely used in signal processing applications such as modeling and feature extraction [89]. It is considered a parametric spectral estimation method, in contrast to non-parametric techniques like PSD or the FT. LP is especially preferred when analyzing ERG signals with a limited number of samples, where traditional methods may not provide sufficient information. When the signal duration is long enough, the FT can be used to estimate the number of poles in the system. One of the main advantages of LP is its ability to accurately identify the dominant frequencies in short-duration signals. This allows for simultaneous detection of frequency changes and efficient data compression [90].

5.2.4 Comparison of studies based on frequency approaches

As outlined in Table 4, frequency-domain analyses, using FT, PSD, and LP, provided more precise quantification of retinal responses, particularly at specific frequency ranges between 6–100 Hz. These studies revealed that reductions in high-frequency components could serve as early markers of cone dysfunction and glaucoma damage. Despite the improved signal stability and enhanced sensitivity of newer techniques such as LED-based PERGx, most research relied on limited datasets and cross-sectional designs, which restrict longitudinal interpretation of frequency alterations.

5.3 Time-frequency nalysis

Time-frequency analysis (TFA) is a technique used to study the spectral changes of a signal over time. Time-frequency analysis can easily distinguish between signal components that may have the same frequency range but occur at different time points, making it a useful tool for analyzing non-stationary biomedical signals that vary over time [96] .Wavelet transform (WT) are typically applied in both forms to increase the amount of information extracted and improve results [97]. Indices derived from the spectral entropy (power spectrum) and dominant frequencies of the time-frequency waveform are sometimes used to identify the ERG of affected

Table 4. A compilation of all frequency-domain investigations performed on all ERG responses.

Year [Ref]	Signal /Stimulation	No. of Subjects	Feature Extraction	Limitations
2015 [91]	Flickering & current ERG	6 human subjects	FFT (Main frequencies: 12.56 Hz, 50.26 Hz)	Artifacts from electrode movement; filtered for accurate interpretation
2017 [92]	PERGx vs. Pattern Electroretinography for Glaucoma Analysis (PERGLA; Light-Emitting Diode (LED)-based stimuli)	57 (29 localized glaucoma, 10 diffuse glaucoma, 18 healthy controls)	FA temporal adaptation assessment Signal-to-Noise Ratio , SNR) calculation of SS-PERG amplitude and latency measured via LED-based PERGx at 15.63 Hz; response adaptation analyzed over ~2 min.	Conventional Cathode Ray Tube monitors caused response delays; ignored temporal adaptation, limited dynamic range for advanced optic neuropathy cases
٢٠١٨ [93]	Full-field sinusoidal flicker 6–100 Hz	20 healthy controls, 20 eyes with non-proliferative diabetic retinopathy without diabetic retinopathy (NDR), and 20 eyes with mild non-proliferative diabetic retinopathy (mild NPDR).	FFT: amplitude & phase of fundamental component; harmonic analysis	Small sample; cross-sectional design limits tracking progression; PhNR & PERG neglected; weak responses at 100 Hz reduce assessment accuracy
٢٠١٩ [94]	ffERG (Light-adapted single-flash & 30 Hz flicker, short color flashes <1 ms, 2.8–4.0 log Td·s)	60 eyes (20 healthy, 20 NDR, 20 mild NPDR)	Log Rmp3 & log S from a-wave (delayed Gaussian model); flicker ERG amplitudes from time-frequency analysis; OPs from 70–300 Hz filtering	A cross-sectional design prevents tracking progression over time or inferring causality
2019 [95]	FERG + PERG	12 people (6 normal, 6 POAG stages I & II)	Fourier Series + Polynomial Amplitude-Frequency Characteristics (AFC)	Very small sample size (6 normal, 6 POAG)

patients[98]. Various transforms have been used to extract features that describe changes in a signal across both time and frequency. A summary of time-frequency-based ERG investigations is presented in Table 5.

5.3.1 Short-Time Fourier Transform

STFT is an essential technique for the time-frequency analysis, which works by separating the signal into tiny time windows and performing the Fourier transform on each one independently. This method FT allows for the observation of how the frequency content of a signal changes over time [98,99]. The resulting output is typically presented as a two-dimensional representation, where the horizontal axis corresponds to time, the vertical axis to frequency, and the signal amplitude is encoded using color gradients. The resolution of the STFT in the frequency domain depends on the window length: longer windows provide higher frequency resolution but lower time resolution, while shorter windows offer better time localization at the cost of reduced frequency resolution. This inherent compromise, known as the time-frequency trade-off, is one of the main limitations of STFT [١٠٠], as it prevents simultaneous optimization in both domains. The choice and design of the window function also significantly influence the analysis outcome, as windows help reduce unwanted artifacts such as the Gibbs phenomenon, which arises from the abrupt truncation of the signal and leads to artificial components in the frequency spectrum. Proper windowing helps suppress these side lobes, enhancing the accuracy of spectral interpretation [100,101,102].

$$X_{STFT}(\tau\ f) = \int_{-\infty}^{\infty} x(t)\, g^{*(t-\tau)e^{-j2\pi ft}} dt \qquad (3)$$

Where g (t) represents the window used, and τ represents the time offset.

5.3.2 Wavelet analysis (WA)

WT is a powerful and effective method and one of the most widely used methods for time-frequency analysis. It is particularly important when dealing with non-stationary signals, such as biomedical signals, whose frequencies vary over time [95,98]. There are two basic types of WT: CWT and DWT [١٠٣,١٠٤]. WT is usually applied in both forms to increase the amount of information extracted and improve and achieve better results [97].CWT is a powerful and flexible analytical tool. It is considered a technique for examining non-stationary time series data. Where it is used a variable-length analysis window that adapts to frequency. This allows for high resolution at low frequencies, while short windows are used for high-frequency analysis, providing a more accurate and time-varying assessment. Unlike the STFT, which uses a fixed-length analysis window, [106]. Furthermore, the CWT does not rely exclusively on traditional representations in the time and frequency domain; it operates on a time scale that can be converted to a time-frequency domain using a pseudo-frequency, the center frequency of each waveform used in the analysis.This transform offers tremendous

flexibility, as it does not require sinusoidal functions and does not impose strict mathematical constraints on the signals studied, unlike traditional Fourier analysis. This versatility makes it applicable to a wide variety of signal types. People think that CWT is the best way to find small and fast changes in time, and it works very well for looking at local features in a signal.

The following formula defines the CWT, which represents the correlation between the continuous-time signal x (t) under analysis and a function known as wavelets [107].

$$CW(a,b) = \int_{-\infty}^{+\infty} x(t)\psi_{a,b}{}^{*}\,dt \qquad (4)$$
$$= \frac{1}{\sqrt{a}}\int_{-\infty}^{+\infty} x(t)\psi^{*}\left(\frac{t-b}{a}\right)dt$$

Where the function of parameters a and b is denoted by CWT (a,b), ψ*(t) is the complex conjugate of the analyzing mother wavelet ψ(t), and b specifies a translation of the wavelet and shows the temporal localization. The parameter a is the wavelet's dilatation (scale) [107,108]. The energy-normalized factor, or coefficient $\frac{1}{\sqrt{a}}$ requires that the wavelet's energy be constant throughout a range of scale values. Moreover, a wavelet function must meet the following mathematical requirements to be categorized as a fundamental acceptable wavelet .[109,110]

The second type is the DWT, which has high processing speed and accuracy, making it suitable for signal classification and data compression applications [109]. Therefore, time-domain analysis of retinal function should be complemented by DWT descriptors, especially in difficult diagnostic cases [112].DWT can be implemented as a filter set of high-pass and low-pass filters, along with up-sampling and down-sampling operations. In the DWT coefficient equation is given by the following equation is given [113].

$$DWT(j,k) = \frac{1}{\sqrt{2j}}\int_{-\infty}^{+\infty} x(t)\,\psi\left(\frac{t-2^{j}k}{2^{j}}\right)dt \qquad (5)$$

5.3.3 Matching pursuit

Matching Pursuit (MP) is an iterative technique that offers effective time-frequency resolution across all frequencies [114]. MP has more flexibility than WA and STFT, since it adjusts the window length based on the local features of the time series [115]. Consequently, MP offers superior temporal and frequency resolution and has been used for diverse signals, including electroencephalography (EEG) and electrocardiography (ECG) [115,116]. The implementation of MP to ERG signals remains in its nascent phase of development. Utilizing an iterative process, MP identifies the signal's representation within a function dictionary, which generally comprises symmetric functions, including Gaussian-modulated sine functions, exemplified by Gabor functions. Employing a time-frequency dictionary of Gabor functions, MP adaptively decomposes the one-dimensional signal into a collection of wavelet atoms. The features of the decomposition may vary depending on the selection of time-frequency atoms, such as Gabor. These waveforms are automatically selected to optimally conform to the signal structures.

Table 5. A compilation of all-time-frequency feature investigations performed on all ERG responses.

Year [Ref]	Signal Stimulation	No. of Subjects	Feature Extraction	Limitations
2014 [19]	Focal Cone ERG, 20° amber LED, 5 Hz	108 (Early AMD n=54, Healthy n=54)	implicit times of the a- and b-waves (descending and ascending phases), amplitude (Amp), Gradients, Frequency domain (5–45 Hz)	Not specified
2015 [24]	Photopic ERG	28 (Normal 18, IIH 10)	Time domain: a,b, PhNR; Frequency domain: DWT, Wavelet Energy; Time-frequency: PhNR reconstruction	Noise removal; CWT complex & redundant → DWT used
2016 [118]	Photopic ERG	61 (Normal 40, Patients 21)	DWT: Amp, time-to-peak (a,b), rise/fall	Weak signals, low SNR; band pass filtering causes distortion; DWT improves accuracy
2016 [119]	ffERG	1 Normal	DWT, CWT, STFT: a,b, i waves, PNR, OPs	Low SNR leads to distortion; CWT is affected by the cone of influence
2017 [120]	Photopic ERG	20 Normal	DWT: PhNR features (Amp at 72 ms, Trough Amp, Energy 11 Hz, 60–120 ms)	Difficult trough identification; DWT complex; weak PhNR-B wave correlation
2017 [121]	ffERG	40 Normal	FFT, DWT, CWT: Amp & peak time (a,b), frequency& spectral features	Time domain limited; sensitive to noise; subtle changes may be missed

2019 [122]	2F-mfERG	60 (Healthy 35, POAG 25)	DWT: variance, energy, median, min, max, Standard Deviation(SD), Interquartile Range	Small sample; central retina only; unbalanced age/sex; advanced glaucoma not included
2020 [123]	PERG	60 (Healthy 30, POAG 30)	DWT: mean, SD, relative energy (detail & approximation L6-7); wavelets: db4, db8, sym5, sym7, coif5	Small sample; subtle variations hard to assess clinically
2020 [124]	ffERG	34 (Normal 17, Central Retinal Vein Occlusion (CRVO) 17)	CWT: Amp & peak times (a,b, PhNR), dominant frequency f0–f3, occurrence t0–t3	Small sample; single disease CRVO; single analysis technique
٢٠٢١ [125]	SS-PERG	45 (Glaucoma 28, Healthy 17)	Amp & phase per packet, slope, phase dispersion, grand-average vector	Small sample; only right eye; confounders not considered
2021 [70]	ffERG	40	Time domain: Amp & peak (a,b); Time-Frequency: STFT, CWT (Mexican Hat), DWT	Small sample; limits generalizability (e.g., obesity effects)
٢٠٢٢ [126]	PERG	53 (Normal 29, Major Depressive Disorder (MDD) 24)	DWT, Principal Component Analysis (PCA), Minimum Covariance Determinant: Amp & implicit time (P50,N95), wavelet features	Small sample; age/gender differences; treatments not evaluated separately
2022 [127]	ffERG (photopic-scotopic, OPs)	425 (pediatric & adult)	CWT + machine learning (ML), such as Decision Tree algorithms	Limited database; reliance on Gaussian wave
2023 [128]	ffERG (Max, Scotopic, Photopic)	323 patients, 1975 signals (Pediatric)	CWT: Ricker, Gaussian, Morlet	Data unbalanced; resampling used
2023 [129]	ffERG (Max, Scotopic, Photopic)	351 (after balancing)	CWT: Shannon, Ricker, Morlet, Gaussian, Complex Gaussian	Single device (Tomey EP-1000) limits generalizability; noise; protocols limited; retinal dystrophy only
2024 [130]	ffERG (Max, Scotopic, Photopic)	322 patients, 1975 signals	Time: a,b Amp & implicit time; Freq: FT; Time-Freq: Spectrogram & STFT (bmin,bmax,bmedian,bmean)	ML limited to 4 features; manual extraction bias; unbalanced data
2024 [131]	ffERG (scotopic, photopic)	120 (after balancing)	4 manually extracted features	Small dataset; limited features
٢٠٢٥ [132]	mfERG (103 hexagons)	2 (Healthy 1, Congenital Stationary Night Blindness(CSNB) 1)	Time-Freq signatures, frequency energy, temporal indices, waveform shape	Reduced accuracy at signal edges; mother wavelet choice affects results; CWT more computationally intensive than DWT

5.3.4 Comparison of studies based on time–frequency approaches

As summarized in Table 5, time–frequency analysis of ERG signals has evolved into a comprehensive framework that enhances early detection of retinal dysfunction. Studies between 2014 and 2025 progressively integrated temporal and frequency information through methods such as FFT, DWT, CWT, and STFT, achieving superior characterization of a, b-, and PhNR components compared with conventional time- or frequency-only analyses. Wavelet-based techniques, particularly DWT and CWT, demonstrated improved sensitivity to subtle functional alterations and reduced signal distortion, while recent combinations with deep learning models (e.g., ResNet, DenseNet) achieved classification accuracies exceeding 88%. These advancements highlight the potential of hybrid analytical approaches that combine ERG signal processing with artificial intelligence (AI) for early diagnosis and clinical decision support. Nevertheless, variations in protocols, small sample sizes, and the computational complexity of CWT remain major challenges for routine clinical application.

Collectively, these analytical approaches demonstrate the progressive evolution of ERG signal processing from basic temporal characterization to multi-domain analyses incorporating spectral and time–frequency information. The discussion that follows critically compares these methods and outlines their clinical and research implications.

6. Comparative Analysis and Future Prospects

A comparative evaluation of analytical domains reveals clear distinctions in their diagnostic performance and applicability. Time-domain methods remain simple and clinically accessible, providing direct indicators such as amplitude and

implicit time that are easy to interpret but limited in sensitivity to subtle functional alterations. Frequency-domain techniques, while offering higher precision through spectral decomposition, are constrained by noise sensitivity and the need for standardized acquisition protocols. In contrast, time–frequency approaches, particularly wavelet-based analyses, capture transient and localized changes with superior accuracy, supporting the detection of early neuronal or vascular dysfunctions. From a practical standpoint, integrating time–frequency features with OCT or AI-based classifiers is recommended for future research, as this combination enhances both diagnostic specificity and automation potential. Clinically, adopting hybrid analytical frameworks could improve early screening protocols for glaucoma, diabetic retinopathy, and hereditary retinal dystrophies, facilitating more objective and quantitative monitoring of disease progression.

7. Conclusion

This review demonstrates that ERG signal analysis has evolved from relying on traditional time-domain properties, such as amplitude and latency, to using more sophisticated techniques in the frequency and time-frequency domains. In time-domain analysis, studies have focused on basic indicators of retinal function, but limited sample sizes and small signal sizes have limited generalizability. Frequency analysis using tools such as FFT, PSD, and PERGx has allowed for more accurate characterization of frequency components, but variability in protocols and the difficulty of exploiting high frequencies such as 50 Hz have been limitations. In contrast, time-frequency analysis using wavelets (WT, CWT, and DWT) has provided a better characterization of dynamic changes in signals, but the computational complexity and difficulty in selecting the optimal wavelet remain practical challenges. Therefore, combining time-frequency characteristics and electroretinography analysis with advanced imaging techniques, such as optical OCT, along with machine learning and artificial neural networks for feature extraction, represents a promising direction toward developing accurate and effective diagnostic tools capable of early detection of retinal diseases and better monitoring their progression.

References

[1] E. Y. Chew, “Summary Results and Recommendations From the Age-Related Eye Disease Study,” *Archives of Ophthalmology*, vol. 127, no. 12, p. 1678, Dec. 2009, doi: 10.1001/archophthalmol.2009.312.

[2] S. Aumann, S. Donner, J. Fischer, and F. Müller, “Optical Coherence Tomography (OCT): Principle and Technical Realization,” in *High Resolution Imaging in Microscopy and Ophthalmology*, Springer International Publishing, 2019, pp. 59–85. doi: 10.1007/978-3-030-16638-0_3.

[3] D. C. Hood *et al.*, “Detecting glaucoma with only OCT: Implications for the clinic, research, screening, and AI development,” *Prog Retin Eye Res*, vol. 90, p. 101052, Sep. 2022, doi: 10.1016/j.preteyeres.2022.101052.

[4] B. L. Sikorski, G. Malukiewicz, J. Stafiej, H. Lesiewska-Junk, and D. Raczynska, “The diagnostic function of OCT in diabetic maculopathy,” *Mediators Inflamm*, vol. 2013, 2013, doi: 10.1155/2013/434560.

[5] E. E. Cornish, A. Vaze, R. V. Jamieson, and J. R. Grigg, “The electroretinogram in the genomics era: outer retinal disorders,” Sep. 01, 2021, *Springer Nature*. doi: 10.1038/s41433-021-01659-y.

[6] V. Porciatti, “Electrophysiological assessment of retinal ganglion cell function,” Nov. 20, 2014, *Academic Press*. doi: 10.1016/j.exer.2015.05.008.

[7] G. Querques, F. Bandello, R. Sacconi, L. Querques, E. Corbelli, and M. V. Cicinelli, “Recent advances in the management of dry age-related macular degeneration: A review,” 2017, *Faculty of 1000 Ltd*. doi: 10.12688/f1000research.10664.1.

[8] S. S. M. Sheet, T.-S. Tan, M. A. As’ari, W. H. W. Hitam, and J. S. Y. Sia, “Retinal disease identification using upgraded CLAHE filter and transfer convolution neural network,” *ICT Express*, vol. 8, no. 1, pp. 142–150, Mar. 2022, doi: 10.1016/j.icte.2021.05.002.

[9] Leonard A. Levin, Paul L. Kaufman, and Mary Elizabeth Hartnett, *Adler’s Physiology of the Eye (E-book)*, 12th ed. Elsevier Health Sciences, 2024.

[10] Stephen L. Polyak, *The Retina*. Chicago, IL, USA: University of Chicago Press, 1941.

[11] D. J. Creel, “Electroretinograms,” 2019, pp. 481–493. doi: 10.1016/B978-0-444-64032-1.00032-1.

[12] D. G. Birch, “Quantitative Electroretinogram Measures of Phototransduction in Cone and Rod Photoreceptors,” *Archives of Ophthalmology*, vol. 120, no. 8, p. 1045, Aug. 2002, doi: 10.1001/archopht.120.8.1045.

[13] D. C. Hood and D. G. Birch, “A quantitative measure of the electrical activity of human rod photoreceptors using electroretinography,” *Vis Neurosci*, vol. 5, no. 04, pp. 379–387, Oct. 1990, doi: 10.1017/S0952523800000468.

[14] R. Barraco, D. Persano Adorno, L. Bellomonte, and M. Brai, “A study of the human rod and cone electroretinogram a-

wave component," *Journal of Statistical Mechanics: Theory and Experiment*, vol. 2009, no. 3, 2009, doi: 10.1088/1742-5468/2009/03/P03007.

[15] J. R. ; A. G. B. Heckenlively, *Principles and Practice of Clinical Electrophysiology of Vision*. St. Louis: Mosby-Year Book, Inc., 1991.

[16] M. B. Hoffmann *et al.*, "ISCEV standard for clinical multifocal electroretinography (mfERG) (2021 update)," *Documenta Ophthalmologica*, vol. 142, no. 1, pp. 5–16, Feb. 2021, doi: 10.1007/s10633-020-09812-w.

[17] D. A. Thompson, M. Bach, J. J. McAnany, M. Šuštar Habjan, S. Viswanathan, and A. G. Robson, "ISCEV standard for clinical pattern electroretinography (2024 update)," *Documenta Ophthalmologica*, vol. 148, no. 2, pp. 75–85, Apr. 2024, doi: 10.1007/s10633-024-09970-1.

[18] A. G. Robson *et al.*, "ISCEV Standard for full-field clinical electroretinography (2022 update)," Jun. 01, 2022, *Springer Science and Business Media Deutschland GmbH*. doi: 10.1007/s10633-022-09872-0.

[19] A. Wood, T. Margrain, and A. M. Binns, "Detection of early age-related macular degeneration using novel functional parameters of the focal cone electroretinogram," *PLoS One*, vol. 9, no. 5, May 2014, doi: 10.1371/journal.pone.0096742.

[20] M. Nebbioso, R. Grenga, and P. Karavitis, "Early Detection of Macular Changes With Multifocal ERG in Patients on Antimalarial Drug Therapy," *Journal of Ocular Pharmacology and Therapeutics*, vol. 25, no. 3, pp. 249–258, Jun. 2009, doi: 10.1089/jop.2008.0106.

[21] D. C. Hood, L. J. Frishman, S. Saszik, and S. Viswanathan, "Retinal Origins of the Primate Multifocal ERG: Implications for the Human Response," *Invest Ophthalmol Vis Sci*, vol. 43, pp. 1673–1685, May 2002, doi: 10.1167/iovs.02-0192.

[22] D. C. Hood, "Assessing retinal function with the multifocal technique," *Prog Retin Eye Res*, vol. 19, no. 5, pp. 607–646, Sep. 2000, doi: 10.1016/S1350-9462(00)00013-6.

[23] H. H. Chan, Y. Ng, and P. H. Chu, "Applications of the multifocal electroretinogram in the detection of glaucoma," *Clin Exp Optom*, vol. 94, no. 3, pp. 247–258, May 2011, doi: 10.1111/j.1444-0938.2010.00571.x.

[24] Hansa Kundra, "Measurement of the Photopic Negative Response of the Electroretinogram by Discrete Wavelet Analysis," University of Illinois Chicago, 2015. [Online]. Available: https://hdl.handle.net/10027/19651

[25] Alan V. Oppenheim, Brian R. Musicus, and Jae S. Lim, "Digital Signal Processing," Cambridge, MA, 1987. [Online]. Available: https://dspace.mit.edu/bitstream/handle/1721.1/57007/RLE_PR_129_24.pdf

[26] M. Azarmina, "Full-Field versus Multifocal Electroretinography," *J Ophthalmic Vis Res*, vol. 8, no. 3, pp. 191–192, Jul. 2013.

[27] E. E. Sutter and D. Tran, "The field topography of ERG components in man—I. The photopic luminance response," *Vision Res*, vol. 32, no. 3, pp. 433–446, Mar. 1992, doi: 10.1016/0042-6989(92)90235-B.

[28] Graham E Holder, "The pattern electroretinogram in anterior visual pathway dysfunction and its relationship to the pattern visual evoked potential: A personal clinical review of 743 eyes," *Eye*, vol. 11, pp. 924–934, Jan. 1997.

[29] G. E. Holder, "Pattern Electroretinography (PERG) and an Integrated Approach to Visual Pathway Diagnosis," *Prog Retin Eye Res*, vol. 20, no. 4, pp. 531–561, Jul. 2001, doi: 10.1016/S1350-9462(00)00030-6.

[30] S. Kara and A. Güven, "Training a learning vector quantization network using the pattern electroretinography signals," *Comput Biol Med*, vol. 37, no. 1, pp. 77–82, Jan. 2007, doi: 10.1016/j.compbiomed.2005.10.005.

[31] G. E. Holder, M. G. Brigell, M. Hawlina, T. Meigen, Vaegan, and M. Bach, "ISCEV standard for clinical pattern electroretinography - 2007 update," *Documenta Ophthalmologica*, vol. 114, no. 3, pp. 111–116, May 2007, doi: 10.1007/s10633-007-9053-1.

[32] V. Porciatti and L. M. Ventura, "Normative Data for a User-friendly Paradigm for Pattern Electroretinogram Recording," *Ophthalmology*, vol. 111, no. 1, pp. 161–168, 2004, doi: 10.1016/j.ophtha.2003.04.007.

[33] O. Ozdamar, J. Toft-Nielsen, J. Bohorquez, and V. Porciatti, "Relationship Between Transient and Steady-State Pattern Electroretinograms: Theoretical and

Experimental Assessment," *Invest Ophthalmol Vis Sci*, vol. 55, no. 12, pp. 8560–8570, Dec. 2014, doi: 10.1167/iovs.14-15685.

[34] D. L. McCulloch *et al.*, "ISCEV Standard for full-field clinical electroretinography (2015 update)," *Documenta Ophthalmologica*, vol. 130, no. 1, Jan. 2015, doi: 10.1007/s10633-014-9473-7.

[35] A. G. Robson *et al.*, "ISCEV guide to visual electrodiagnostic procedures," *Documenta Ophthalmologica*, vol. 136, no. 1, pp. 1–26, Feb. 2018, doi: 10.1007/s10633-017-9621-y.

[36] P. A. ; M. K. ; N. F. Seiving, "Push-pull model of primate photopic electroretinogram: The role of hyperpolarizing neurons in the formation of the b-wave," *Vis Neurosci*, vol. 11, no. 3, 2009.

[37] Laura J. Frishman and Minhua H. Wang, "Electroretinogram of human, monkey and mouse," in *Adler's Physiology of the Eye*, 11th ed., Leonard A. Levin, Siv F. E. Nilsson, James Ver Hoeve, Samuel M. Wu, and Albert Alm, Eds., Elsevier Saunders, 2011, pp. 480–501.

[38] Lillemor Wachtmeister, "Basic research and clinical aspects of the oscillatory potentials of the electroretinogram," *Documenta Ophthalmologica*, vol. 66, no. 3, pp. 187–194, Jun. 1987, doi: 10.1007/BF00145232.

[39] T. E. Ogden, "The oscillatory waves of the primate electroretinogram," *Vision Res*, vol. 13, no. 6, pp. 1059-IN4, Jun. 1973, doi: 10.1016/0042-6989(73)90144-2.

[40] S. ; F. L. Viswanathan, "Evidence that negative potentials in the photopic electroretinograms of cats and primates depend upon spiking activity of retinal ganglion cell axons," vol. 23, p. 1024, 1997.

[41] R. A. Bush and P. A. Sieving, "Inner retinal contributions to the primate photopic fast flicker electroretinogram," *Journal of the Optical Society of America A*, vol. 13, no. 3, p. 557, Mar. 1996, doi: 10.1364/JOSAA.13.000557.

[42] J. G. Robson and L. J. Frishman, "The rod-driven a-wave of the dark-adapted mammalian electroretinogram," 2014, *Elsevier Ltd*. doi: 10.1016/j.preteyeres.2013.12.003.

[43] Y. Bhatt, D. M. Hunt, and L. S. Carvalho, "The origins of the full-field flash electroretinogram b-wave," 2023, *Frontiers Media SA*. doi: 10.3389/fnmol.2023.1153934.

[44] Y. B. Younis and F. Al Azzo, "Integrative detection of retinal detachment with AlexNet and heat maps visualization," *Math Appl*, vol. 13, no. 1, pp. 110–123, 2024, doi: 10.13164/ma.2024.13108.

[45] V. T. S. Tang, R. C. A. Symons, S. Fourlanos, D. Guest, and A. M. McKendrick, "The relationship between ON–OFF function and OCT structural and angiographic parameters in early diabetic retinal disease," *Ophthalmic and Physiological Optics*, vol. 45, no. 1, pp. 77–88, Jan. 2025, doi: 10.1111/opo.13394.

[46] A. Mavilio, F. Scrimieri, and D. Errico, "Can variability of pattern ERG signal help to detect retinal ganglion cells dysfunction in glaucomatous eyes?," *Biomed Res Int*, vol. 2015, 2015, doi: 10.1155/2015/571314.

[47] C. W. Huang *et al.*, "The structure–function correlation analysed by OCT and full field ERG in typical and pericentral subtypes of retinitis pigmentosa," *Sci Rep*, vol. 11, no. 1, Dec. 2021, doi: 10.1038/s41598-021-96570-7.

[48] K. Dhaliwal, A. Wong, T. Wright, and K. Bizheva, "Combined optical coherence tomography and electroretinography system for imaging neurovascular coupling in the human retina," *Neurophotonics*, vol. 12, no. 03, Aug. 2025, doi: 10.1117/1.nph.12.3.035004.

[49] S. Yang *et al.*, "Photoreceptor dysfunction in early and intermediate age-related macular degeneration assessed with mfERG and spectral domain OCT," *Documenta Ophthalmologica*, vol. 132, no. 1, pp. 17–26, Feb. 2016, doi: 10.1007/s10633-016-9523-4.

[50] K. Park, J. Kim, and J. Lee, "Measurement of macular structure-function relationships using spectral domain-optical coherence tomography (SD-OCT) and pattern electroretinograms (PERG)," *PLoS One*, vol. 12, no. 5, May 2017, doi: 10.1371/journal.pone.0178004.

[51] M. Unlu, D. Gulmez Sevim, M. Gultekin, and C. Karaca, "Correlations among multifocal electroretinography and optical coherence tomography findings in patients with Parkinson's disease," *Neurological Sciences*, vol. 39, no. 3, pp. 533–541, Mar. 2018, doi: 10.1007/s10072-018-3244-2.

[52] L. Frizziero *et al.*, "Early retinal changes by oct angiography and multifocal electroretinography in diabetes," *J Clin Med*, vol. 9, no. 11, Nov. 2020, doi: 10.3390/jcm9113514.

[53] S. Y. Lee, N. H. Son, H. W. Bae, G. J. Seong, and C. Y. Kim, "The role of pattern electroretinograms and optical coherence tomography angiography in the diagnosis of normal-tension glaucoma," *Sci Rep*, vol. 11, no. 1, Dec. 2021, doi: 10.1038/s41598-021-91813-z.

[54] B. Cvenkel, M. Sustar, and D. Perovšek, "Monitoring for glaucoma progression with SAP, electroretinography (PERG and PhNR) and OCT," *Documenta Ophthalmologica*, vol. 144, no. 1, pp. 17–30, Feb. 2022, doi: 10.1007/s10633-021-09854-8.

[55] H. Komatsu *et al.*, "Retina as a potential biomarker in schizophrenia spectrum disorders: a systematic review and meta-analysis of optical coherence tomography and electroretinography," Feb. 01, 2024, *Springer Nature*. doi: 10.1038/s41380-023-02340-4.

[56] E. J. Ahn, Y. I. Shin, Y. K. Kim, J. W. Jeoung, and K. H. Park, "Hemifield-based analysis of pattern electroretinography in normal subjects and patients with preperimetric glaucoma," *Sci Rep*, vol. 14, no. 1, Dec. 2024, doi: 10.1038/s41598-024-55601-9.

[57] D. A. Thompson *et al.*, "Predicting OCT retinal ganglion cell volume from pattern ERGs and VEPs in children with suspected optic neuropathy in a tertiary referral setting," *BMJ Open Ophthalmol*, vol. 10, no. 1, Mar. 2025, doi: 10.1136/bmjophth-2024-001899.

[58] M. Gauvin, J. M. Lina, and P. Lachapelle, "Advance in ERG analysis: From peak time and amplitude to frequency, power, and energy," *Biomed Res Int*, vol. 2014, 2014, doi: 10.1155/2014/246096.

[59] Z. M. Tariq and M. S. Jarjees, "Localized Muscle Fatigue Prediction and Detection Using Surface Electromyography: A Review Study 1."

[60] H. Ahmadieh, S. Behbahani, and S. Safi, "Continuous wavelet transform analysis of ERG in patients with diabetic retinopathy," *Documenta Ophthalmologica*, vol. 142, no. 3, pp. 305–314, Jun. 2021, doi: 10.1007/s10633-020-09805-9.

[61] Z. Wu, L. N. Ayton, R. H. Guymer, and C. D. Luu, "Comparison between multifocal electroretinography and microperimetry in age-related macular degeneration," *Invest Ophthalmol Vis Sci*, vol. 55, no. 10, pp. 6431–6439, 2014, doi: 10.1167/iovs.14-14407.

[62] R. W. Jansson, M. B. Raeder, and J. Krohn, "Photopic full-field electroretinography and optical coherence tomography in type 1 diabetic retinopathy," *Graefe's Archive for Clinical and Experimental Ophthalmology*, vol. 253, no. 7, pp. 989–997, Jul. 2015, doi: 10.1007/s00417-015-3034-y.

[63] K. Deák, I. Fejes, M. Janáky, T. Várkonyi, G. Benedek, and G. Braunitzer, "Further Evidence for the Utility of Electrophysiological Methods for the Detection of Subclinical Stage Retinal and Optic Nerve Involvement in Diabetes," *Medical Principles and Practice*, vol. 25, no. 3, pp. 282–285, Apr. 2016, doi: 10.1159/000442163.

[64] M. Gao *et al.*, "Assessment of macular function in patients with idiopathic Epiretinal membrane by multifocal Electroretinography: Correlation with visual acuity and optical coherence tomography," *BMC Ophthalmol*, vol. 17, no. 1, Nov. 2017, doi: 10.1186/s12886-017-0621-1.

[65] J. Karaśkiewicz, K. Penkala, M. Mularczyk, and W. Lubiński, "Evaluation of retinal ganglion cell function after intraocular pressure reduction measured by pattern electroretinogram in patients with primary open-angle glaucoma," *Documenta Ophthalmologica*, vol. 134, no. 2, pp. 89–97, Apr. 2017, doi: 10.1007/s10633-017-9575-0.

[66] S. Patangay *et al.*, "Three dimensional stimulus source for pattern electroretinography in mid- and far-peripheral retina," *Transl Vis Sci Technol*, vol. 7, no. 1, 2018, doi: 10.1167/tvst.7.1.8.

[67] T. Salgarello *et al.*, "Pattern electroretinogram detects localized glaucoma defects," *Transl Vis Sci Technol*, vol. 7, no. 5, Sep. 2018, doi: 10.1167/tvst.7.5.6.

[68] M. Kim, R. Y. Kim, W. Park, Y. G. Park, I. B. Kim, and Y. H. Park, "Electroretinography and retinal microvascular changes in type 2 diabetes," *Acta Ophthalmol*, vol. 98, no. 7, pp. e807–e813, Nov. 2020, doi: 10.1111/aos.14421.

[69] M. Tabl, "Early detection of neurodegeneration in type 2 diabetic patients without diabetic retinopathy using electroretinogram and spectral-domain optical coherence tomography," *Journal of the Egyptian Ophthalmological Society*, vol. 113, no. 1, p. 26, 2020, doi: 10.4103/ejos.ejos_72_19.

[70] O. Erkaymaz, Í. Senyer Yapici, and R. Uzun Arslan, "Effects of obesity on time-frequency components of electroretinogram signal using continuous wavelet transform," *Biomed Signal Process Control*, vol. 66, p. 102398, Apr. 2021, doi: 10.1016/j.bspc.2020.102398.

[71] S. Bakhshi, S. Behbahani, and N. Daftarian, "Application of a Mapping Method in the Analysis of Electroretinogram in Patients with Retinitis Pigmentosa," *Semin Ophthalmol*, vol. 37, no. 3, pp. 351–357, 2022, doi: 10.1080/08820538.2021.1967411.

[72] B. Cvenkel, M. Sustar, and D. Perovšek, "Monitoring for glaucoma progression with SAP, electroretinography (PERG and PhNR) and OCT," *Documenta Ophthalmologica*, vol. 144, no. 1, pp. 17–30, Feb. 2022, doi: 10.1007/s10633-021-09854-8.

[73] A. A. Alhagaa, N. M. Badawi, and O. A. A. El-Morsy, "Primary Open Angle Glaucoma Diagnosis Using Pattern Electroretinogram Parameters," *Clinical Ophthalmology*, vol. 17, pp. 3281–3293, 2023, doi: 10.2147/OPTH.S424323.

[74] C. Huchzermeyer, R. Lämmer, C. Y. Mardin, F. E. Kruse, J. Kremers, and F. K. Horn, "Pattern electroretinogram, blue-yellow visual evoked potentials and the risk of developing visual field defects in glaucoma suspects: a longitudinal 'survival' analysis with a very long follow-up," *Graefe's Archive for Clinical and Experimental Ophthalmology*, vol. 262, no. 5, pp. 1607–1618, May 2024, doi: 10.1007/s00417-023-06364-y.

[75] B. Karaman, A. Öner, and A. Güven, "Early detection and staging of retinitis pigmentosa using multifocal electroretinogram parameters and machine learning algorithms," *Phys Eng Sci Med*, 2025, doi: 10.1007/s13246-025-01577-3.

[76] A. Güven, B. Karaman, A. Öner, and N. Sinim Kahraman, "Detection of retinitis pigmentosa stages with GAN and transfer learning in maps of MfERG P1 wave amplitudes," *Signal Image Video Process*, vol. 19, no. 7, p. 528, Jul. 2025, doi: 10.1007/s11760-025-04111-w.

[77] T. Salgarello *et al.*, "Steady-State PERG Adaptation Reveals Temporal Abnormalities of Retinal Ganglion Cells in Treated Ocular Hypertension and Glaucoma," *Diagnostics*, vol. 15, no. 14, Jul. 2025, doi: 10.3390/diagnostics15141797.

[78] R. Barraco, D. Persano Adorno, M. Brai, and L. Tranchina, "A comparison among different techniques for human ERG signals processing and classification," *Physica Medica*, vol. 30, no. 1, pp. 86–95, Feb. 2014, doi: 10.1016/j.ejmp.2013.03.006.

[79] M. Gur and Y. Zeevi, "Frequency-domain analysis of the human electroretinogram," *J Opt Soc Am*, vol. 70, no. 1, p. 53, Jan. 1980, doi: 10.1364/JOSA.70.000053.

[80] A. Bagheri, D. Persano Adorno, P. Rizzo, R. Barraco, and L. Bellomonte, "Empirical mode decomposition and neural network for the classification of electroretinographic data," *Med Biol Eng Comput*, vol. 52, no. 7, pp. 619–628, 2014, doi: 10.1007/s11517-014-1164-8.

[81] H. Hassan-Karimi, E. Jafarzadehpur, B. Blouri, H. Hashemi, A. Z. Sadeghi, and A. Mirzajani, "Frequency Domain Electroretinography in Retinitis Pigmentosa versus Normal Eyes," *J. Ophthalmic Vis. Res.*, vol. 7, no. 1, pp. 34–38, 2012, [Online]. Available: https://www.ncbi.nlm.nih.gov/pmc/articles/PMC3381106/

[82] M. Bach *et al.*, "ISCEV standard for clinical pattern electroretinography (PERG): 2012 update," *Documenta Ophthalmologica*, vol. 126, no. 1, pp. 1–7, Feb. 2013, doi: 10.1007/s10633-012-9353-y.

[83] W. van Drongelen, *Signal Processing for Neuroscientists*. Amsterdam: Academic Press, 2018.

[84] R. N. Youngworth, B. B. Gallagher, and B. L. Stamper, "An overview of power spectral density (PSD) calculations," in *Optical Manufacturing and Testing VI*, SPIE, Aug. 2005, p. 58690U. doi: 10.1117/12.618478.

[85] D. D. Arianandа and G. Leus, "Compressive wideband power spectrum estimation," *IEEE Transactions on Signal Processing*, vol. 60, no. 9, pp. 4775–4789, 2012, doi: 10.1109/TSP.2012.2201153.

[86] A. S. Al-Fahoum and A. A. Al-Fraihat, "Methods of EEG Signal Features Extraction Using Linear Analysis in Frequency and Time-Frequency Domains," *ISRN Neurosci*, vol. 2014, pp. 1–7, Feb. 2014, doi: 10.1155/2014/730218.

[87] P. Welch, "The use of fast Fourier transform for the estimation of power spectra: A method based on time averaging over short, modified periodograms," *IEEE Transactions on Audio and Electroacoustics*, vol. 15, no. 2, pp. 17–19, Jun. 1967, doi: 10.1109/TAU.1967.1161901.

[88] Alan V. Oppenheim and G. Verghese, "Power Spectral Density," in *Signals, Systems and Inference*, 1st ed., Cambridge, MA: Massachusetts Institute of Technology, 2010, ch. 10, pp. 183–194. [Online]. Available: https://ocw.mit.edu/courses/electrical-engineering-and-computer-science/6-011-introduction-to-communication-control-and-signal-processing-spring-2010/

[89] P. P. Vaidyanathan, "The theory of linear prediction," *Synthesis Lectures on Signal Processing*, vol. 3, pp. 1–181, Jan. 2007, doi: 10.2200/S00086ED1V01Y200712SPR03.

[90] H. Baali, A. Khorshidtalab, M. Mesbah, and M. J. E. Salami, "A Transform-Based Feature Extraction Approach for Motor Imagery Tasks Classification," *IEEE J Transl Eng Health Med*, vol. 3, 2015, doi: 10.1109/JTEHM.2015.2485261.

[91] C. Pahl, N. B. Mohammad, and E. Supriyanto, "Analysis on the electroretinography response for flickering and current stimulations," in *2015 38th International Conference on Telecommunications and Signal Processing, TSP 2015*, Institute of Electrical and Electronics Engineers Inc., Oct. 2015, pp. 482–485. doi: 10.1109/TSP.2015.7296309.

[92] P. Monsalve *et al.*, "Next generation PERG method: Expanding the response dynamic range and capturing response adaptation," *Transl Vis Sci Technol*, vol. 6, no. 3, May 2017, doi: 10.1167/tvst.6.3.5.

[93] J. J. McAnany and J. C. Park, "Temporal frequency abnormalities in early-stage diabetic retinopathy assessed by electroretinography," *Invest Ophthalmol Vis Sci*, vol. 59, no. 12, pp. 4871–4879, Oct. 2018, doi: 10.1167/iovs.18-25199.

[94] J. J. McAnany and J. C. Park, "Cone photoreceptor dysfunction in early-stage diabetic retinopathy: Association between the activation phase of cone phototransduction and the flicker electroretinogram," *Invest Ophthalmol Vis Sci*, vol. 60, no. 1, pp. 64–72, Jan. 2019, doi: 10.1167/iovs.18-25946.

[95] Z. M. Vladimirovna, "Assessment of the Amplitude-Frequency Characteristics of the Retina with Its Stimulation by Flicker and Chess Pattern-Reversed Incentives and their Use to Obtain New Formalized Signs of Retinal Pathologies," *Biomed J Sci Tech Res*, vol. 19, no. 5, Jul. 2019, doi: 10.26717/bjstr.2019.19.003358.

[96] P. Flandrin, *Time-Frequency and Time-Scale Analysis*. New York: Academic Press, 1999.

[97] A. Alaql, "Analysis and Processing of Human Electroretinogram," M.S. Thesis, University of South Florida, Tampa, FL, 2016. [Online]. Available: http://scholarcommons.usf.edu/etd/6059

[98] S. S. Nair and K. Paul Joseph, "Wavelet based electroretinographic signal analysis for diagnosis," *Biomed Signal Process Control*, vol. 9, pp. 37–44, Jan. 2014, doi: 10.1016/j.bspc.2013.09.008.

[99] Lokenath Debnath, *Wavelets and Signal Processing*. Springer Science & Business Media, 2003.

[100] M. G. E. Schneiders, "Wavelets in control engineering," Ph.D. Dissertation, Eindhoven University of Technology, Eindhoven, 2001.

[101] S. Nisar, O. U. Khan, and M. Tariq, "An Efficient Adaptive Window Size Selection Method for Improving Spectrogram Visualization," *Comput Intell Neurosci*, 2016, doi: 10.1155/2016/6172453.

[102] S. Yu *et al.*, "STFT-like time frequency representations of nonstationary signal with arbitrary sampling schemes," *Neurocomputing*, vol. 204, pp. 211–221, Sep. 2016, doi: 10.1016/j.neucom.2015.08.130.

[103] Z. Lin and J. D. Z. Chen, "Advances in Time-Frequency Analysis of Biomedical Signals," *Crit Rev Biomed Eng*, vol. 24, no. 1, pp. 1–72, 1996, doi: 10.1615/CritRevBiomedEng.v24.i1.10.

[104] T. Rogala and A. Brykalski, "Wavelet feature space in computer-aided electroretinogram evaluation," *Pattern*

Analysis and Applications, vol. 8, no. 3, pp. 238–246, Dec. 2005, doi: 10.1007/s10044-005-0003-9.

[105] J. Rafiee, M. A. Rafiee, N. Prause, and M. P. Schoen, "Wavelet basis functions in biomedical signal processing," *Expert Syst Appl*, vol. 38, no. 5, pp. 6190–6201, May 2011, doi: 10.1016/j.eswa.2010.11.050.

[106] O. Rioul, M. Vetterli, and M. V. Wavelets, "and signal processing," 1991. [Online]. Available: https://telecom-paris.hal.science/hal-03330354v1

[107] D. Komorowski and S. Pietraszek, "The Use of Continuous Wavelet Transform Based on the Fast Fourier Transform in the Analysis of Multi-channel Electrogastrography Recordings," *J Med Syst*, vol. 40, no. 1, Jan. 2016, doi: 10.1007/s10916-015-0358-4.

[108] A.-H. Najmi, J. Sadowsky, A.-H. Najmi, and J. Sadowsky, "The continuous wavelet transform and variable resolution time-frequency analysis," *Johns Hopkins APL Tech Dig*, vol. 18, no. 1, pp. 134–140, 1997.

[109] "Table of contents," *IEEE Engineering in Medicine and Biology Magazine*, vol. 28, no. 5, pp. 1–2, Sep. 2009, doi: 10.1109/MEMB.2009.934235.

[110] R. Merry, "Wavelet theory and applications." [Online]. Available: www.tue.nl/taverne

[111] S. G. Mallat, "A Theory for Multiresolution Signal Decomposition: The Wavelet Representation," Philadelphia, PA, USA, May 1987.

[112] M. Gauvin, H. Chakor, R. K. Koenekoop, J. M. Little, J.-M. Lina, and P. Lachapelle, "Witnessing the first sign of retinitis pigmentosa onset in the allegedly normal eye of a case of unilateral RP: a 30-year follow-up," *Documenta Ophthalmologica*, vol. 132, no. 3, pp. 213–229, Jun. 2016, doi: 10.1007/s10633-016-9537-y.

[113] A. F. Hussein, S. J. Hashim, A. F. A. Aziz, F. Z. Rokhani, and W. A. W. Adnan, "Performance Evaluation of Time-Frequency Distributions for ECG Signal Analysis," *J Med Syst*, vol. 42, no. 1, p. 15, Jan. 2018, doi: 10.1007/s10916-017-0871-8.

[114] G. Liu *et al.*, "Complexity Analysis of Electroencephalogram Dynamics in Patients with Parkinson's Disease," *Parkinsons Dis*, vol. 2017, 2017, doi: 10.1155/2017/8701061.

[115] M. Wacker and H. Witte, "Time-frequency techniques in biomedical signal analysis: A tutorial review of similarities and differences," *Methods Inf Med*, vol. 52, no. 4, pp. 279–296, 2013, doi: 10.3414/ME12-01-0083.

[116] H. ZHANG, C. CHEN, Y. WU, and P. LI, "Decomposition and compression for ECG and EEG signals with sequence index coding method based on matching pursuit," *The Journal of China Universities of Posts and Telecommunications*, vol. 19, no. 2, pp. 92–95, Apr. 2012, doi: 10.1016/S1005-8885(11)60251-3.

[117] C. Baumgartner *et al.*, "Discussion of 'Time-frequency Techniques in Biomedical Signal Analysis: A Tutorial Review of Similarities and Differences,'" *Methods Inf Med*, vol. 52, no. 04, pp. 297–307, Jan. 2013, doi: 10.1055/s-0038-1627059.

[118] M. Gauvin *et al.*, "Assessing the Contribution of the Oscillatory Potentials to the Genesis of the Photopic ERG with the Discrete Wavelet Transform," *Biomed Res Int*, vol. 2016, 2016, doi: 10.1155/2016/2790194.

[119] H. Kundra, J. C. Park, and J. J. McAnany, "Comparison of photopic negative response measurements in the time and time–frequency domains," *Documenta Ophthalmologica*, vol. 133, no. 2, pp. 91–98, Oct. 2016, doi: 10.1007/s10633-016-9558-6.

[120] M. Gauvin, A. L. Dorfman, and P. Lachapelle, "Recording and Analysis of the Human Clinical Electroretinogram," 2018, pp. 313–325. doi: 10.1007/978-1-4939-7522-8_23.

[121] M. Gauvin and B. Eng, "Time-frequency analysis of the human photopic electroretinogram: method, normative data and clinical applications," Montréal, 2017.

[122] L. M. Brandao, M. Monhart, A. Schötzau, A. A. Ledolter, and A. M. Palmowski-Wolfe, "Wavelet decomposition analysis in the two-flash multifocal ERG in early glaucoma: a comparison to ganglion cell analysis and visual field," *Documenta Ophthalmologica*, vol. 135, no. 1, pp. 29–42, Aug. 2017, doi: 10.1007/s10633-017-9593-y.

[123] H. Hassankarimi, S. M. R. Noori, E. Jafarzadehpour, S. Yazdani, and F. Radinmehr, "Analysis of pattern electroretinogram signals of early primary open-angle glaucoma in coefficients

domain," *Int Ophthalmol*, vol. 39, no. 10, pp. 2373–2383, Oct. 2019, doi: 10.1007/s10792-019-01077-w.

[124] S. Behbahani, A. Ramezani, M. Karimi Moridani, and H. Sabbaghi, "Time-Frequency Analysis of Photopic Negative Response in CRVO Patients," *Semin Ophthalmol*, vol. 35, no. 3, pp. 187–193, Apr. 2020, doi: 10.1080/08820538.2020.1781905.

[125] T. Salgarello *et al.*, "PERG adaptation for detection of retinal ganglion cell dysfunction in glaucoma: a pilot diagnostic accuracy study," *Sci Rep*, vol. 11, no. 1, Dec. 2021, doi: 10.1038/s41598-021-02048-x.

[126] T. Schwitzer *et al.*, "Retinal electroretinogram features can detect depression state and treatment response in adults: A machine learning approach," *J Affect Disord*, vol. 306, pp. 208–214, Jun. 2022, doi: 10.1016/j.jad.2022.03.025.

[127] A. Zhdanov, A. Dolganov, D. Zanca, V. Borisov, and M. Ronkin, "Advanced Analysis of Electroretinograms Based on Wavelet Scalogram Processing," *Applied Sciences (Switzerland)*, vol. 12, no. 23, Dec. 2022, doi: 10.3390/app122312365.

[128] M. Kulyabin, A. Zhdanov, A. Dolganov, M. Ronkin, V. Borisov, and A. Maier, "Enhancing Electroretinogram Classification with Multi-Wavelet Analysis and Visual Transformer," *Sensors (Basel)*, vol. 23, no. 21, Oct. 2023, doi: 10.3390/s23218727.

[129] M. Kulyabin, A. Zhdanov, A. Dolganov, and A. Maier, "Optimal Combination of Mother Wavelet and AI Model for Precise Classification of Pediatric Electroretinogram Signals," *Sensors*, vol. 23, no. 13, Jul. 2023, doi: 10.3390/s23135813.

[130] F. B. Albas, "Analysis and Classification of Full-Field Electroretinogram Signals," 2024.

[131] F. Albasu *et al.*, "Electroretinogram Analysis Using a Short-Time Fourier Transform and Machine Learning Techniques," *Bioengineering*, vol. 11, no. 9, Sep. 2024, doi: 10.3390/bioengineering11090866.

[132] Y. Shwetar, D. Lalush, J. McAnany, B. Jeffrey, and M. Haendel, "A Practical Introduction to Wavelet Analysis in Electroretinography," Jul. 27, 2025. doi: 10.1101/2025.07.25.25331915.